# ECOGRAPHY

*Research*

# Improving landscape-scale productivity estimates by integrating trait-based models and remotely-sensed foliar-trait and canopy-structural data

Daniel J. Wieczynski, Sandra Díaz, Sandra M. Durán, Nikolaos M. Fyllas, Norma Salinas, Roberta E. Martin, Alexander Shenkin, Miles R. Silman, Gregory P. Asner, Lisa Patrick Bentley, Yadvinder Malhi, Brian J. Enquist and Van M. Savage

D. J. Wieczynski (https://orcid.org/0000-0003-4090-2677) ✉ (daniel.wieczynski@duke.edu) and V. M. Savage (https://orcid.org/0000-0003-3639-3718), Dept of Ecology and Evolutionary Biology, Univ. of California, Los Angeles, Los Angeles, CA, USA. DJW also at: Dept of Biology, Duke Univ., Durham, NC, USA. – S. Díaz (https://orcid.org/0000-0003-0012-4612), Consejo Nacional de Investigaciones Científicas y Técnicas, Inst. Multidisciplinario de Biología Vegetal (IMBIV) and Facultad de Ciencias Exactas, Físicas y Naturales, Univ. Nacional de Córdoba, Córdoba, Argentina. – S. M. Durán (https://orcid.org/0000-0003-2044-8139) and B. J. Enquist (https://orcid.org/0000-0002-6124-7096), Dept of Ecology and Evolutionary Biology, Univ. of Arizona, Tucson, AZ, USA. – N. M. Fyllas (https://orcid.org/0000-0002-5651-5578), Biodiversity Conservation Laboratory, Dept of Environment, Univ. of the Aegean, Mytilene, Greece. – N. Salinas (https://orcid.org/0000-0001-9941-2109), Inst. for the Sciences of Nature, Earth and Energy (INTE-PUCP), Pontifical Catholic Univ. of Peru, Lima, Peru. – R. E. Martin (https://orcid.org/0000-0003-3509-8530) and G. P. Asner (https://orcid.org/0000-0001-7893-6421), School for Geographical Sciences and Urban Planning and Center for Global Discovery and Conservation Science, Arizona State Univ., Tempe, AZ, USA. – A. Shenkin (https://orcid.org/0000-0003-2358-9367) and Y. Malhi (https://orcid.org/0000-0002-3503-4783), Environmental Change Inst., School of Geography and the Environment, Univ. of Oxford, Oxford, UK. – M. R. Silman, Dept of Biology and Center for Energy, Environment and Sustainability, Wake Forest Univ., Winston-Salem, NC, USA. – L. P. Bentley (https://orcid.org/0000-0002-6180-8842), Dept of Biology, Sonoma State Univ., Rohnert Park, CA, USA. BJE and VMS also at: Santa Fe Inst., Santa Fe, NM, USA.

Assessing the impacts of anthropogenic degradation and climate change on global carbon cycling is hindered by a lack of clear, flexible and easy-to-use productivity models along with scarce trait and productivity data for parameterizing and testing those models. We provide a simple solution: a mechanistic framework (RS-CFM) that combines remotely-sensed foliar-trait and canopy-structural data with trait-based metabolic theory to efficiently map productivity at large spatial scales. We test this framework by quantifying net primary productivity (NPP) at high-resolution (0.01-ha) in hyper-diverse Peruvian tropical forests (30040 hectares) along a 3322-m elevation gradient. Our analysis captures hotspots and elevational shifts in productivity more accurately and in greater detail than alternative empirical- and process-based models that use plant functional types. This result exposes how high-resolution, location-specific variation in traits and light competition drive variability in productivity, opening up possibilities to fully harness remote sensing data and reliably scale up from traits to map global productivity in a more direct, efficient and cost-effective manner.

Keywords: climate, functional biogeography, productivity, remote sensing, trait-based ecology, tropical forests

## Introduction

Forests are essential to the earth's active carbon cycle (Field et al. 1998, Pan et al. 2011) but their future is uncertain under the current threats of anthropogenic degradation and climate change, especially in the tropics (Grace et al. 2014, Schimel et al. 2015, Baccini et al. 2017, Mitchard 2018). Accurately predicting the consequences of these global threats will require understanding how plant functional traits scale up to influence whole-forest productivity (Violle et al. 2014, Enquist et al. 2015). Trait-based theory and metabolic theory have shown that morphological, architectural and chemical traits – such as plant height, biomass, leaf area index (LAI), wood density, leaf mass per unit area (LMA) and leaf foliar chemistry (nitrogen, phosphorus and carbon content) – directly influence individual plant growth rates, survival, and, in turn, forest productivity (Wright et al. 2004, Enquist et al. 2007, 2015, Violle et al. 2007, Adler et al. 2014, Díaz et al. 2016, Funk et al. 2017, Fyllas et al. 2017). In addition, the collection of functional traits expressed within forests varies substantially with changes in geography and climate (Violle et al. 2014, Šímová et al. 2015, Bruelheide et al. 2018, Wieczynski et al. 2019). Currently, we have an opportunity to capture trait composition and diversity at finer resolutions and larger spatial scales than ever before through remote sensing (RS). However, current ecosystem models still use coarse functional groupings that might not represent trait variation at the individual level. It is therefore crucial to take advantage of these technological and theoretical advances that more directly link traits, plant growth and shifts in functional trait composition across environments to uncover the forces that drive variation in carbon flux across space and time.

Relationships between functional trait composition and ecosystem processes have been difficult to discern for two main reasons. First, it is challenging to accurately and comprehensively measure the functional trait composition of forests, especially at large spatial scales and remote or difficult-to-sample locations (Newbold et al. 2012). Solving this problem is the great promise of remote sensing (RS) technology – using airborne or satellite imaging to collect extensive, high-resolution data at local, regional or global scales (Vane and Goetz 1988, Green et al. 1998, Ustin et al. 2004, Aplin 2005, Gillespie et al. 2008, de Araujo Barbosa et al. 2015, Houborg et al. 2015). Remote sensing has created a surge of information about the functional trait characteristics of forests (Aplin 2005, Chambers et al. 2007, de Araujo Barbosa et al. 2015, Houborg et al. 2015), leading to important ecological insights about foliar chemistry (Asner and Martin 2016, Lausch et al. 2016), forest canopy structure (Lim et al. 2003, Zimble et al. 2003), taxonomic and functional diversity (Nagendra 2001, Asner et al. 2017, Schneider et al. 2017, Durán et al. 2019, Wang and Gamon 2019), biomass and carbon stocks (Lu 2006, Goetz and Dubayah 2011) and relationships between functional traits and productivity (Smith et al. 2002, Hilker et al. 2008, Song et al. 2013). These discoveries have resulted in previous initiatives to integrate remotely-sensed functional trait data with vegetation growth models (Homolová et al. 2013, Scheiter et al. 2013, Fisher et al. 2018, Boisvenue and White 2019) – for example, dynamic global vegetation models (DGVMs) like LPJ-DGVM (Sitch et al. 2003) and ED2 (Medvigy et al. 2009) – to better assess spatiotemporal variation in carbon storage/flux across scales.

The second challenge is that many previous studies that relate remotely-sensed forest data to productivity do so via either empirical (statistical) models or intricate process-based models. Empirical models estimate productivity using proxies of plant growth like chlorophyll (Madani et al. 2017), nitrogen (Smith et al. 2002), light use efficiency (LUE) (Hilker et al. 2008) or the normalized difference vegetation index (NDVI) (Running et al. 2004, Zhao et al. 2005). Process-based models like DGVMs and individual-based forest simulators are often extremely complex, requiring up to hundreds of parameters, many sub-models and considerable computational power and time (Purves and Pacala 2008, Strigul et al. 2008, Scheiter et al. 2013, Larocque et al. 2016, Fisher et al. 2018). Extrapolating the results of purely empirical models to new systems and climates can be hazardous because they lack mechanistic linkages among traits, plant growth and productivity. Instead, they rely on statistical relationships between plant growth proxies and productivity within a given dataset (Fisher et al. 2018, Boisvenue and White 2019). DGVMs and forest simulators often require specialized expertise, extensive data inputs or special access (Larocque et al. 2016), making them hard to implement or reproduce for most researchers. In such models, functional traits are rarely collected remotely and are usually coarsely represented as plant functional types rather than species- or individual-level traits (Purves and Pacala 2008, Fisher et al. 2018, Boisvenue and White 2019). Moreover, competition for light is often only roughly incorporated (Purves and Pacala 2008, Quillet et al. 2010, Scheiter et al. 2013, Yang et al. 2015), although models including forest demographics (Sitch et al. 2003, Medvigy et al. 2009, Fisher et al. 2018) or variation in canopy light availability through radiative transfer (Pury and Farquhar 1997, Kattge et al. 2009, Bonan et al. 2012, Fyllas et al. 2017, Fauset et al. 2019) can accommodate more realistic light environments.

The empirical and process-based models outlined above offer highly-detailed productivity calculations for a range of resolutions and situations, providing productivity maps at the regional and global scale based on physiological processes and at least moderate functional detail. However, a simpler, more mechanistic approach to growth models that utilizes remotely-sensed functional trait data could be a complementary alternative to current productivity models that provides greater functional detail as well as a fundamental basis for understanding which factors are most important for driving variation in productivity (Klausmeier et al. 2020). These factors can then be varied within such models to estimate productivity in new systems or changes in productivity with changes in climate or forest composition/structure. This endeavor has been dubbed the 'Holy Grail' of plant functional ecology (Lavorel and Garnier 2002), but has remained elusive for the reasons outlined above.

Here we introduce a new remote sensing canopy functional model (RS-CFM, Fig. 1) that overcomes both data and modeling challenges by merging remote sensing data with trait-based metabolic theory (Enquist et al. 2007). Our RS-CFM makes several notable advances on current approaches by:

- *More accurately representing on-the-ground functional variation* via incorporation of high-resolution, location-specific functional-trait and canopy-structural data collected remotely, as opposed to less precise information based on plant functional types.
- *Simplifying productivity computation* to make it faster, easier to manipulate and explore parameter space, easier to clarify relationships between plant traits and productivity, and more open and accessible such that any individual can run it using their own data on their own computer (i.e. without a supercomputer).
- *Scaling up from individual-level processes to ecosystem-level patterns* by mechanistically linking traits and performance, thus addressing the need for theory-based and hypothesis-driven models that incorporate traits to predict vegetation growth and ecosystem processes.

We use this framework to address three specific questions: 1) Does combining trait-based metabolic theory with remote-sensing data accurately capture variation in productivity across environmental gradients? 2) Is accuracy improved by using high-resolution, location-specific functional trait data, as opposed to plant functional types? 3) Are productivity estimates more accurate when we include pixel-level variation in canopy structure and light availability?

As a case study and proof of concept, we evaluate how forest functional trait composition affects variation in NPP in 30 040 hectares of tropical rainforest along a 3322-m elevation gradient in Peru. Our study area spans a mean annual temperature gradient of ~15°C from the lowland Amazonian rainforest to montane forest in the high Andes. Originally established by the Andes Biodiversity and Ecosystem Research Group (ABERG; <www.andesconservation.org>), this site provides a uniquely rich dataset including highly-detailed, ground-based net primary productivity (NPP) measurements (Malhi et al. 2017), ground-based plant functional trait data collected from trees (Asner et al. 2017, Malhi et al. 2017), ground-based NPP model estimates based on this tree functional trait data (Fyllas et al. 2017), and airborne lidar and imaging spectroscopy providing remote-sensing estimates of functional traits and canopy structure (Asner et al. 2015, 2017). Additionally, NPP estimates using alternative empirical (NASA's MODIS NPP product (Zhao et al. 2005)) and process-based (Breathing Earth System Simulator (BESS)) (Ryu et al. 2011, Jiang and Ryu 2016) approaches also exist for this region. This region and dataset thus provide a unique opportunity to fully evaluate our RS-CFM along a broad environmental gradient and in the context of known productivity measurements and a range of alternative productivity models.

Our results demonstrate that remotely-sensed trait data can be reliably scaled up to predict variation in productivity – significantly outperforming alternative methods. This opens up possibilities to take advantage of a rapidly-growing inventory of remote data (Kampe et al. 2010, Lee et al. 2015, Asner and Martin 2016, Müller et al. 2016, Gamon et al. 2019, Dubayah et al. 2020) and fulfill the current need for a framework that quantifies productivity across regions in a more direct, efficient and cost-effective manner (Boisvenue and White 2019).

## Methods

### Ground-based NPP measurements and model estimates

Our ground-based dataset consists of nine 1-ha forest plots situated along a 3322-m Amazon to Andes elevation transect in Peru. All ground data used in this study were collected in previous field campaigns (Fyllas et al. 2017, Malhi et al. 2017). Collection methods and analyses for ground-based NPP measurements and model estimates are described in detail in the original articles and are summarized here. Ground-based NPP measurements were originally reported by Malhi et al. (2017) for all nine focal plots in the current study and include data collected from 2007 to 2015. Total NPP for each plot was calculated as an aggregate of multiple key components of the autotrophic carbon cycle, including canopy litterfall, leaf loss to herbivory, aboveground woody productivity and branch turnover. Ground-based NPP model estimates were originally calculated for each of these plots by Fyllas et al. (2017) using trait data collected via conventional field measurements of individual trees (no remote sensing data; Malhi et al. 2017). Within each plot, species identity was determined for all stems greater than 10 cm in diameter at breast height (DBH). Trait data were collected for a subset of these individual stems (~7%), including measurements of wood density (WD), leaf dry mass per unit wet area (LMA) and leaf nitrogen (N) and phosphorus (P) content per unit area. These data were then incorporated into an individual-based forest simulator to estimate NPP according to a trait-based vegetation growth equation (Enquist et al. 2007). The ground-based NPP model estimates presented here were recalculated using the same field measurements and an updated version of the original Fyllas et al. model (Fyllas et al. 2017) (described in detail in the Supporting information). The essential advances of our new remote-sensing framework (described below; Fig. 1) over this previous ground-based model (Fyllas et al. 2017) is that we 1) digitally reconstruct the forest canopy using highly-detailed remote-sensing data for traits and canopy structure – instead of using ground-based data collected from trees – and 2) reconfigure the trait-based vegetation growth equation from Enquist et al. (2007) to quantify productivity for individual pixels within this digital forest canopy.

### Remote sensing canopy functional model (RS-CFM)

Our framework quantifies productivity through four basic steps (Fig. 1). First, airborne remote sensing data were collected by the Global Airborne Observatory using visible-to-shortwave infrared (VSWIR) spectrometry and dual-laser
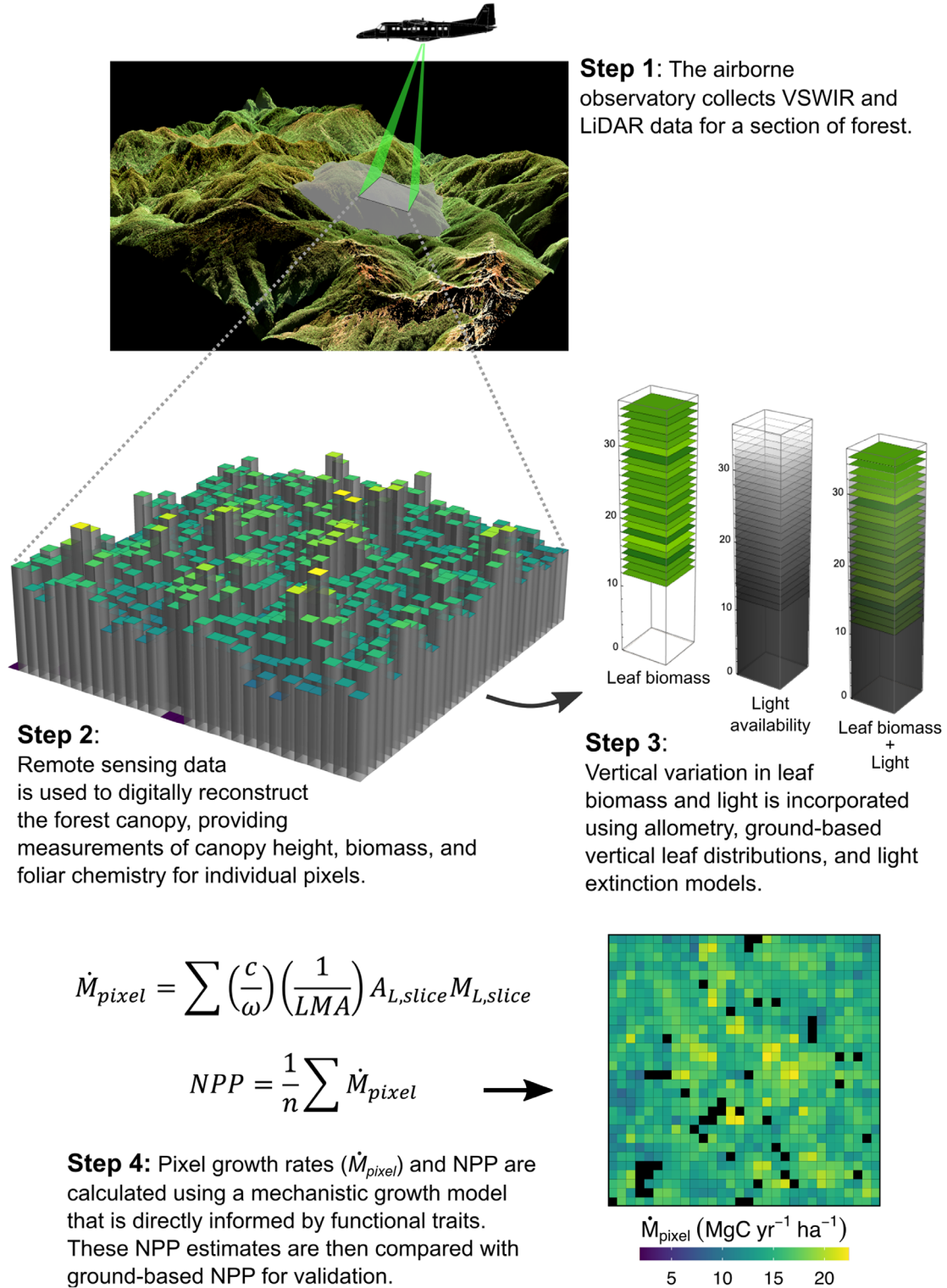
**Step 1**: The airborne observatory collects VSWIR and LiDAR data for a section of forest.

**Step 2**: Remote sensing data is used to digitally reconstruct the forest canopy, providing measurements of canopy height, biomass, and foliar chemistry for individual pixels.

**Step 3**: Vertical variation in leaf biomass and light is incorporated using allometry, ground-based vertical leaf distributions, and light extinction models.

$$\dot{M}_{pixel} = \sum \left(\frac{c}{\omega}\right)\left(\frac{1}{LMA}\right) A_{L,slice} M_{L,slice}$$

$$NPP = \frac{1}{n}\sum \dot{M}_{pixel}$$

**Step 4**: Pixel growth rates ($\dot{M}_{pixel}$) and NPP are calculated using a mechanistic growth model that is directly informed by functional traits. These NPP estimates are then compared with ground-based NPP for validation.

$\dot{M}_{pixel}$ (MgC yr$^{-1}$ ha$^{-1}$)

Figure 1. Step-by-step process for converting remote sensing data (visible-to-shortwave infrared (VSWIR) spectrometry and dual-laser waveform light detection and ranging (LiDAR)) into net primary productivity (NPP) estimates using our trait-based remote sensing canopy functional model (RS-CFM) framework. Growth rate estimates for individual remote sensing pixels ($\dot{M}_{pixel}$) are based on key functional traits including carbon use efficiency ($c$), carbon mass fraction ($\omega$), leaf mass per unit area ($LMA$), leaf photosynthetic rate ($A_L$) – which is a function of $LMA$ and leaf nitrogen ($N$) and phosphorus ($P$) content – and leaf biomass ($M_L$). Within each pixel, $A_L$ and $M_L$ are further subdivided into 1 m pixel slices to account for vertical gradients light and biomass throughout the canopy (step 3) and productivity is calculated for each pixel using trait-based metabolic scaling theory (step 4).

waveform light detection and ranging (LiDAR) (Asner et al. 2015). Second, VSWIR images were processed and analyzed using partial least squares regression to estimate average values of leaf mass per unit area (LMA) and leaf nitrogen and phosphorus content per unit area ($N_{area}$, $P_{area}$) for the vegetation within individual RS pixels (Asner et al. 2015, 2017). LMA, $N_{area}$ and $P_{area}$ were then used as inputs to calculate leaf photosynthetic rates ($A_L$). For each pixel, LiDAR top-of-canopy height measurements and plot-aggregate allometry (Asner et al. 2012a, Asner and Mascaro 2014) were used to estimate total aboveground biomass and leaf-mass allometry (Fyllas et al. 2017) was used to calculate total leaf biomass ($M_L$). Third, to account for vertical heterogeneity in canopy biomass and light availability, individual pixels were divided vertically into 1-m slices, each of which was assigned a unique value for leaf biomass and solar radiation based on vertical biomass and light profiles calculated using ground data (Supporting information). Finally, using our mechanistic plant growth model (RS-CFM), we calculated pixel-level growth rates ($\dot{M}_{pixel}$) by summing growth estimates across all vertical slices within each pixel at 0.01, 1 and 100 ha spatial resolutions. NPP was then calculated as the average growth rate across all pixels within a given plot or elevation band. The remote-sensing data used in steps 1 and 2 were collected and converted from hyperspectral data to trait values in previous studies (Asner et al. 2015, 2017) while all of the remaining components of the RS-CFM are original contributions of the current study.

### Remote-sensing trait and canopy data

Visible-to-shortwave infrared (VSWIR) spectrometry and dual-laser waveform light detection and ranging (LiDAR) remote-sensing (RS) data were previously collected for 9 focal plots by the Global Airborne Observatory in August of 2013 (Asner et al. 2012b, 2015) (Fig. 1, step 1). Although these data fall within the temporal window of ground-based NPP measurements, we acknowledge that environmental variation within and among years is likely to produce variation in NPP that we may not capture using a single snapshot of RS trait data. However, for the purpose of our study – to more accurately estimate variation in NPP as it emerges from the trait composition of forests that vary in mean annual temperature across elevations – our RS data should be sufficiently representative. Each remote sensing (RS) plot is geographically centered over an associated ground plot (Fyllas et al. 2017, Malhi et al. 2017) and is 9 ha in size. The raw hyperspectral and lidar data were previously processed (Asner et al. 2015) to provide estimates of mean top of canopy height (TCH), LMA, N and P within 10 m pixels (0.01 ha) using a previously developed protocol (Asner et al. 2015, 2017, Asner and Martin 2016) (Fig. 1, step 2). Hyperspectral data were shade-masked by Asner et al. (2015) such that only sunlit portions of the canopies were used to measure spectral profiles for traits. RS trait data were also collected for 30 040 hectares of forest surrounding the 9 focal RS plots. Each landscape-scale RS pixel was assigned to an associated focal plot/elevation according to

whichever focal plot was nearest in elevation, creating exclusive elevation bands across the 3344 m gradient. The 0.01 ha RS data were aggregated at 1 ha resolution for both plot-scale and landscape scale datasets. Additionally, landscape-scale RS data were aggregated at 100 ha resolution for direct comparison with MODIS and BESS NPP estimates.

### Vertical variation in pixel-level leaf biomass and light availability

Each RS pixel was divided vertically into 1 m slices that were assigned unique values for leaf biomass and light availability (Fig. 1, step 3; see Supporting information for details). Total biomass within each pixel was estimated as a function of top of canopy height (TCH) using plot-aggregate allometric scaling (Asner et al. 2012a, Asner and Mascaro 2014). Total leaf biomass was estimated for each pixel ($M_{L,pixel}$) by multiplying the total AGB of each pixel by the leaf mass fraction (LMF) of each associated ground plot (Eqn. S6). We then distributed $M_{L,pixel}$ across 1m slices within each RS pixel according the vertical distribution of leaf biomass calculated for associated ground plots. Light availability for each pixel slice was estimated based on a continuous light-decay function calibrated using vertical distributions of leaf area index (LAI) from associated ground plots (Eqn. S16).

### Net primary productivity (NPP) estimates

The rate of change in biomass over time for each pixel slice was calculated using the mean trait values available for each RS pixel (same values used for each slice within a pixel) (Eq. 1):

$$\frac{dM_{slice}}{dt} = \left(\frac{c}{\omega}\right)\left(\frac{1}{LMA}\right)A_{L,slice}M_{L,slice} \qquad 1$$

where $c$ is carbon use efficiency and was previously observed to be constant throughout this study region (Malhi et al. 2017) ($c = 0.33$, no units), $\omega$ is the whole-plant carbon mass fraction (Martin and Thomas 2011, Asner and Mascaro 2014) ($\omega = 0.48$, no units), $A_{L,slice}$ is leaf area specific photosynthetic rate calculated for each pixel slice (gC m$^{-2}$ y$^{-1}$) and is a function of foliar traits (LMA, N and P; Eqn. S8) and light availability, LMA is leaf mass per unit area (g cm$^{-2}$) and $M_{L,slice}$ is the total leaf biomass within an individual pixel slice (kg). Thus, traits were incorporated into the model both directly (LMA and $M_{L,slice}$) and indirectly via their effects on photosynthetic rate (LMA, N and P). Total growth rate per pixel is the sum of growth across all slices within that pixel (Eq. 2):

$$\dot{M}_{pixel} = \frac{dM_{pixel}}{dt} = \sum \frac{dM_{slice}}{dt} \qquad 2$$

Finally, total annual plot NPP was calculated by taking the mean value of $\dot{M}_{pixel}$ across all RS pixels associated with a given plot/elevation (Eq. 3):

$$\text{NPP} = \frac{1}{n} \sum \dot{M}_{\text{pixel}} \qquad\qquad 3$$

The units for both $\dot{M}_{\text{pixel}}$ and NPP were standardized to MgC ha$^{-1}$ yr$^{-1}$ at all spatial scales and resolutions to enable cross-comparison between all RS productivity estimates, ground-based measurements and ground-based model estimates.

**Trait and $\dot{M}_{\text{pixel}}$ analyses**

Pixel growth rate deviations were calculated by subtracting the associated empirical NPP measurements for a given focal plot/elevation from the RS-CFM NPP estimates. In order to compare NPP estimates from each dataset with empirically measured NPP, we calculated root mean squared deviations (RMSD) between measured and estimated (predicted) NPP values for each plot/elevation as (Eq. 4):

$$\text{RMSD} = \sqrt{E\left(\left(\text{NPP}_{\text{measured}} - \text{NPP}_{\text{predicted}}\right)^2\right)} \qquad 4$$

where $E()$ represents the expected value. To differentiate the contributions of individual RS-CFM growth model components – LMA, $N_{\text{area}}$, $P_{\text{area}}$, $A_L$ and $M_L$ – on pixel-level growth rates ($\dot{M}_{\text{pixel}}$) we performed a main effects multiple linear regression with standardized coefficients. To produce standardized regression coefficients, we centered and rescaled all independent variables (growth model components) prior to analysis by subtracting the means and dividing by their standard deviations. Because correlations between model components could affect the interpretability of regression coefficients, we evaluated multicollinearity and the percentage of total variance ($R^2$) in $\dot{M}_{\text{pixel}}$ that is uniquely explained by each model component. We did this by calculating variance inflation factors and performing a commonality analysis (Ray-Mukherjee et al. 2014) using the R functions 'vif' ('car' package; Fox and Weisberg 2019) and 'regr' ('yhat' package; Nimon et al. 2020) respectively.

We evaluated shifts in the distributions of individual RS-CFM growth model components and $\dot{M}_{\text{pixel}}$ values by first calculating the first four central moments of each variable within each plot/elevation. Relationships between the moments of each variable at each spatial scale and resolution were then evaluated using both linear and quadratic regression analyses. In cases where both linear and quadratic models produced significant fits and AIC scores differed by less than 4 points, the linear model was chosen as the best fit model on the basis of parsimony (fewer parameters).

All data analyses and productivity estimations were performed in R ver. 4.0.0 (<www.r-project.org>).

## Results

We begin by comparing our RS-CFM NPP estimates with ground-based NPP measurements (Malhi et al. 2017) and model NPP estimates using trait data collected from trees on the ground (Fyllas et al. 2017). In general, we found very close agreement between ground- and remote-based NPP (Fig. 2, Supporting information). At both the plot- and landscape-scales, our framework accurately predicts local (within-elevation) NPP as well as characteristic declines in NPP with increasing elevation, including the leveling off of NPP at high elevations (Fig. 2a and b). The highest-resolution plot-scale NPP estimates (RS-CFM Plot 0.01 ha) performed best (Fig. 2a, Supporting information), exhibiting a root mean square deviation (RMSD) between measured and predicted NPP of 1.02, lower than all other datasets, even ground-based model estimates (ground model: RMSD = 1.28). At the level of individual pixels, growth estimates ($\dot{M}_{\text{pixel}}$) from the RS Plot 0.01 ha dataset also performed best, deviating from ground-based NPP measurements by only 0.26 MgC ha$^{-1}$ yr$^{-1}$ on average (Fig. 2c, Supporting information).

Interestingly, we found that NPP estimates are sensitive to the spatial scale and resolution of the remote dataset being used. Within all focal plots/elevations, RS-CFM NPP estimates decline with decreasing pixel resolution (Fig. 2a and b, Supporting information). This results in a systematic, downward shift in NPP-elevation trends at lower resolutions, despite the shapes of these trends remaining relatively unchanged. Higher-resolution (0.01 ha) plot-scale data produced highly accurate NPP estimates (RMSD = 1.02) while lower-resolution data slightly underestimated productivity (RMSD = 1.59) (Fig. 2a), suggesting that the accuracy of NPP estimates increases with pixel resolution. However, at the landscape scale, intermediate resolution (1 ha) NPP estimates are actually closest to NPP measurements (RMSD = 1.08) (Fig. 2b).

We compared our approach with two easily accessible alternative methods for estimating NPP using remote-sensing data: 1) NASA's MODIS terrestrial NPP product (empirical model) (Running et al. 2004, Zhao et al. 2005) and 2) the Breathing Earth System Simulator (BESS, which provides GPP estimates that were converted to NPP here using a carbon use efficiency of 0.33) (process-based model) (Ryu et al. 2011, Jiang and Ryu 2016). MODIS NPP estimates are considerably higher on average than both BESS NPP as well as NPP and pixel growth estimates from our RS-CFM (Fig. 2b and d, Supporting information). This result has been noted before (Jiang and Ryu 2016) and is similar to findings that DGVMs also tend to overestimate biomass (Le Toan et al. 2004). Both MODIS and BESS NPP remain relatively constant across elevations, except for a dramatic decline in MODIS estimates at higher elevations, in contrast to gradual declines across all elevations seen in our RS-CFM (Fig. 2b). Moreover, this sharp decline in MODIS NPP estimates occurs exactly where NPP measurements and our model estimates show a leveling off (3537 m; Fig. 2b), potentially due to canopy sparseness reducing the role of vertical variation in light availability. Interestingly, overestimates in MODIS NPP were contrasted by underestimates in BESS NPP at low elevations (Fig. 2b). At the level of individual pixels, MODIS NPP values were substantially higher on average than measured NPP values, exhibiting a mean pixel growth rate deviation of
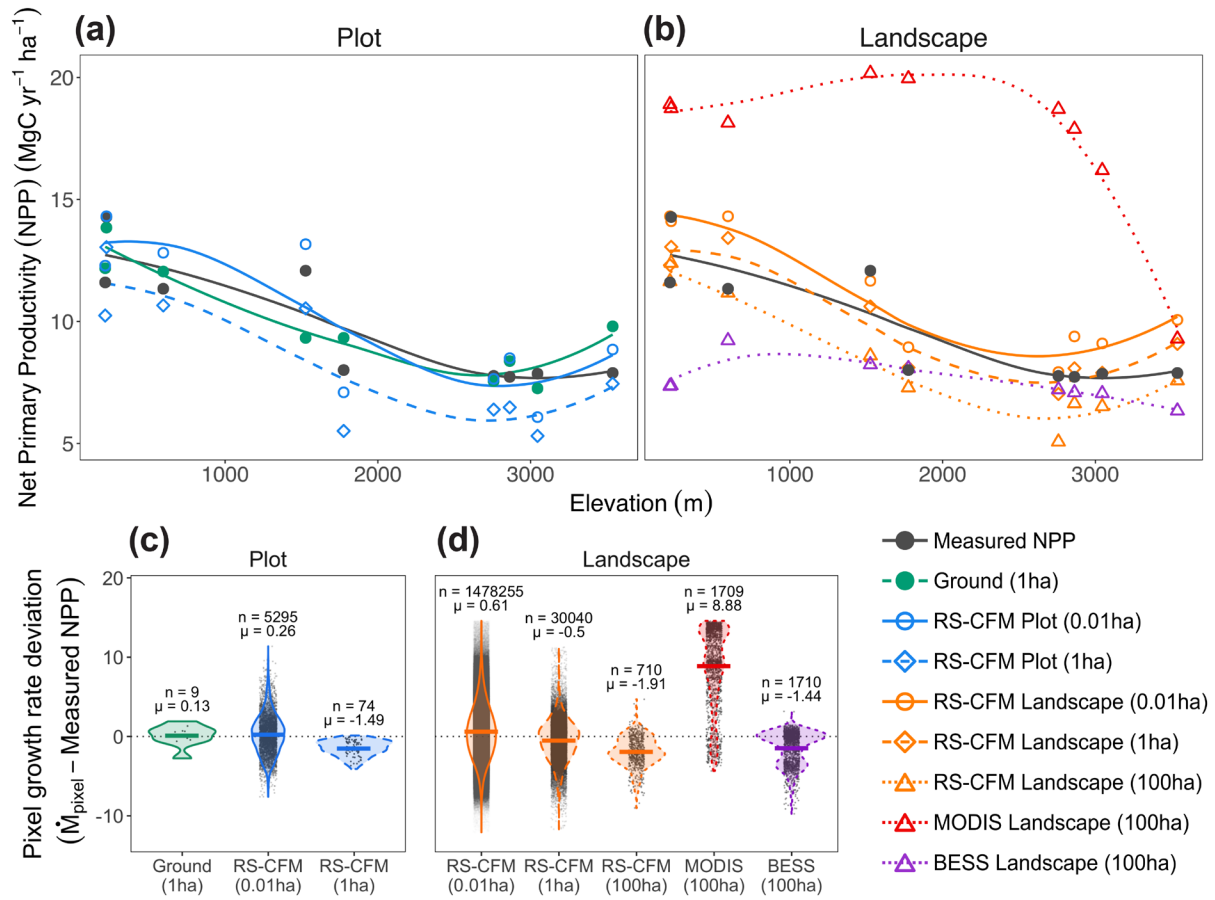
Figure 2. (a–b) Net primary productivity (NPP) and (c–d) individual pixel vegetation growth rate estimates ($\dot{M}_{pixel}$) from ground-based, airborne remote sensing (RS-CFM), NASA-MODIS and BESS NPP models shown at multiple spatial scales (plot and landscape) and resolutions (0.01, 1 and 100 ha). NPP estimates are shown across elevations and compared with ground-based NPP measurements (black) and ground-based NPP model estimates (green) at (a) plot- and (b) landscape-scales. Deviations between pixel growth rate estimates ($\dot{M}_{pixel}$) and NPP measurements at (c) the plot scale and (d) landscape scales. Each gray dot represents the deviation between an individual $\dot{M}_{pixel}$ estimate and the empirical NPP measurement of its associated focal plot and horizontal bars indicate mean values. Note how both mean and variance in $\dot{M}_{pixel}$ deviations tend to decrease with decreasing pixel resolution.

8.88 MgC ha$^{-1}$ yr$^{-1}$ (Fig. 2d). Even at the highest pixel resolution tested here (100 ha), RS-CFM estimates (RMSD = 1.72) represent a significant improvement over both MODIS estimates (RMSD = 8.31) and BESS estimates (RMSD = 3.14) (Supporting information). Indeed, RS-CFM growth estimates were most improved over alternative methods at lower elevations, where the average absolute deviation from empirical NPP measurements was 1.39 MgC ha$^{-1}$ yr$^{-1}$ at 100 ha resolution (0.04 (215 m), −1.89 (223 m), −0.16 (595 m) and −3.48 (1527 m)), compared with 6.66 in MODIS and 4.28 in BESS (Supporting information, Fig. 2b).

The RS-CFM revealed extensive, fine-scale variation in vegetation growth rates at the level of individual pixels ($\dot{M}_{pixel}$). As with NPP estimates, deviations between $\dot{M}_{pixel}$ and associated NPP measurements increased with pixel size (Fig. 2c and d). High-resolution (0.01 ha) plot-scale $\dot{M}_{pixel}$ estimates performed best, exhibiting deviations from measured NPP that were only slightly higher on average than those of ground-based NPP estimates (μ = 0.26 and μ = 0.13 MgC ha$^{-1}$ yr$^{-1}$, respectively; Fig. 2c). Landscape-scale $\dot{M}_{pixel}$

estimates also performed well at both 0.01 ha and 1 ha resolutions (average deviations of μ = 0.61 and μ = −0.50 MgC ha$^{-1}$ yr$^{-1}$, respectively; Fig. 2d). Lower-resolution data resulted in the largest mean pixel growth rate deviations, but this effect was less exaggerated at the landscape scale (Fig. 2c and d). In fact, the mean deviation in $\dot{M}_{pixel}$ at 1 ha resolution was much lower in magnitude at the landscape-scale (μ = −0.50) than at the plot-scale (μ = −1.49) – which was also reflected in the accuracy of associated NPP estimates (plot-scale RMSD = 1.59, landscape-scale RMSD = 1.08; Supporting information). Variation in $\dot{M}_{pixel}$ deviations also increased with pixel resolution and was substantially higher at the landscape scale (Fig. 2c and d, Supporting information), corresponding to wider and more continuous distributions of pixel-level trait values both within and across elevations (Supporting information).

At all scales and resolutions, variation in pixel growth rates is linked to variation in underlying traits. We performed a multiple regression on the individual trait components of our growth model – pixel-level mean LMA, $N_{area}$, $P_{area}$, $A_L$ and

$M_L$ – against $\dot{M}_{pixel}$ values using standardized coefficients to determine which traits had the largest impact on variation in growth rates. At all spatial scales and resolutions, $M_L$, $A_L$ and LMA were the strongest predictors of variance in $\dot{M}_{pixel}$ while leaf nitrogen and phosphorus content, though significant, were less influential (e.g. parameter estimates in the RS-CFM 0.01 ha model were: LMA $= -2.03$, $N_{area} = 0.07$, $P_{area} = 0.23$, $A_L = 2.69$ and $M_L = 2.47$, adjusted $R^2 = 0.92$, p $< 10^{-5}$; Supporting information). Variance inflation factors (VIFs) indicated moderate levels of multicollinearity among traits (i.e. VIF $> 1$), but commonality analysis showed that the variance in $\dot{M}_{pixel}$ explained uniquely by each trait was still highest for $M_L$, $A_L$ and LMA (Supporting information), confirming the results of the regression model. Trait distributions also shift in position and shape along the elevation gradient (Supporting information), consistent with shifts reported in previous research in this region (Asner et al. 2017, Fyllas et al. 2017). However, here we also found associated shifts in the distributions of $\dot{M}_{pixel}$ values across elevations (Supporting information). We summarized these shifts by calculating the first four central moments of $\dot{M}_{pixel}$ distributions and evaluating both linear and polynomial (quadratic) regressions across elevation (Supporting information). Mean $\dot{M}_{pixel}$ values (our measure of NPP) decline significantly with increasing elevation at all spatial scales and resolutions. Variance, skewness and kurtosis in $\dot{M}_{pixel}$ distributions tend to increase with elevation. However, evidence for shifts in these higher moments is somewhat limited, except perhaps at the landscape scale.

One of the most crucial and challenging components of our model is the inclusion of vertical heterogeneity in light availability (light competition) (Fig. 3). Instead of using a single light value for each pixel, our RS-CFM uses a straightforward method for distributing light continuously throughout the canopy. In order to evaluate the importance of this component, we compared our light model with two alternatives that assume no vertical light gradient. When vertical light profiles are held constant and light is assumed to be fully available throughout the canopy (i.e. no light competition), our model overestimates productivity (Fig. 3, 'No shading'). However, if we assume that light availability is limited by shading – determined by leaf area index (LAI) – but is not structured by height (as is true in many current carbon models (Purves and Pacala 2008)), then productivity is substantially underestimated (Fig. 3, 'Average shading'). Accounting for this vertical light gradient avoids the problems with both of the limits above and also considerably improves NPP estimates, regardless of the scale or resolution of remote sensing data (Fig. 2). These results are consistent with previous findings (Fyllas et al. 2017) that light competition does indeed play an essential role in the distribution of tree growth rates and estimates of overall forest productivity.

Estimating growth rates using remote sensing data allows us to create high-resolution productivity maps across large regions at multiple spatial scales (Fig. 4). At the plot scale, we find remarkable fine-grain spatial heterogeneity in growth rate estimates both within and across elevations (Fig. 4a). Landscape-scale data reveal a strong elevation gradient in productivity as well as substantial local variation around this trend (Fig. 4b). Such maps provide precise information about the spatial distributions of traits and vegetation growth, allowing us to more accurately measure shifts in productivity with shifts in environmental conditions and to better identify
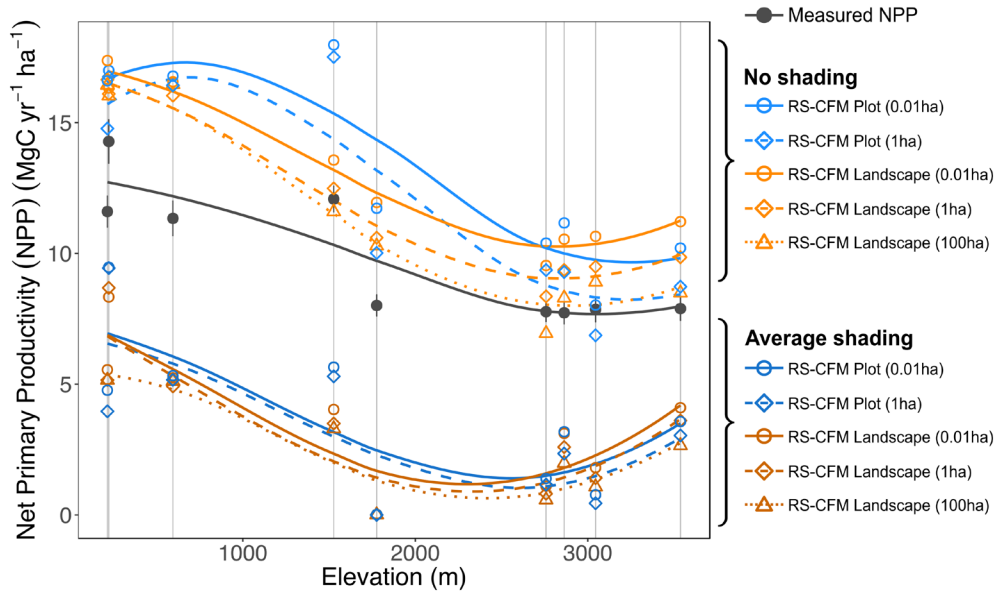


Figure 3. Remote sensing productivity estimates (RS-CFM) calculated using alternative canopy shading schemes. 'No shading' indicates that light is freely available throughout the canopy and 'Average shading' indicates that each vertical canopy slice receives the same amount of light equal to the average throughout a given pixel. Root-mean-square deviation (RMSD) between estimated and measured NPP: no shading plot 3.87 (0.01 ha) 3.02 (1 ha), no shading landscape 3.53 (0.01 ha) 2.73 (1 ha) 2.59 (100 ha), avg. shading plot 6.16 (0.01 ha) 6.51 (1 ha), avg. shading landscape 6.28 (0.01 ha) 6.55 (1 ha) 6.89 (100 ha).

local and regional hotspots in functional diversity and primary production.

## Discussion

Here we combined remotely-sensed trait and canopy data with a mechanistic, trait-based metabolic growth model to estimate productivity at high resolution across large regions and in remote and difficult to sample locations. Our framework is flexible enough to apply to virtually any region or climate because vegetation growth rates are rooted in direct links between a few key plant traits and metabolism (Enquist et al. 2007). This provides a baseline for producing more accurate, location-specific, high-resolution productivity estimates at larger spatial scales and lower costs. This information can be used to better understand the forces governing community assembly and to help predict future shifts in the composition and functioning of forests in response to anthropogenic degradation and climate change. Such an approach is especially crucial in hyper-diverse (Barlow et al. 2018), structurally complex (Gough et al. 2019) productivity hotspots like tropical forests (Field et al. 1998, Roy et al. 2001), where we need to account for detailed and localized functional variation to reduce the high uncertainty in carbon flux predictions with future climate change (Pan et al. 2011, Barlow et al. 2018, Mitchard 2018).

By incorporating highly-localized, fine-grained functional trait and canopy information – as opposed to using plant functional types – we are able to uncover three new and important ecological results:

- Hotspots and shifts in productivity can be identified and mapped with greater accuracy and detail using local trait data, especially at low elevations where the canopy is denser and light competition may be more important (see Fig. 2b and Supporting information (RMSDs of 1.72 for our (RS-CFM) compared with 8.31 (MODIS) and 3.14 (BESS)) and high-resolution (0.01 ha) landscape maps in Fig. 4).
- The accuracy of NPP estimates increases with pixel resolution, reflecting increased variation in location-specific, pixel-level trait values and growth rates (see means and variances in Fig. 2c and d and increased variance in trait/growth rate distributions in Supporting information).
- Productivity estimation is vastly improved when light competition is driven by continuous variation in vertical canopy structure at the level of individual pixels (see Fig. 3 (RMSDs of 1.02 (RS-CFM) compared to 3.87 (no shading) and 6.16 (avg. shading) at 0.01 ha-resolution)).

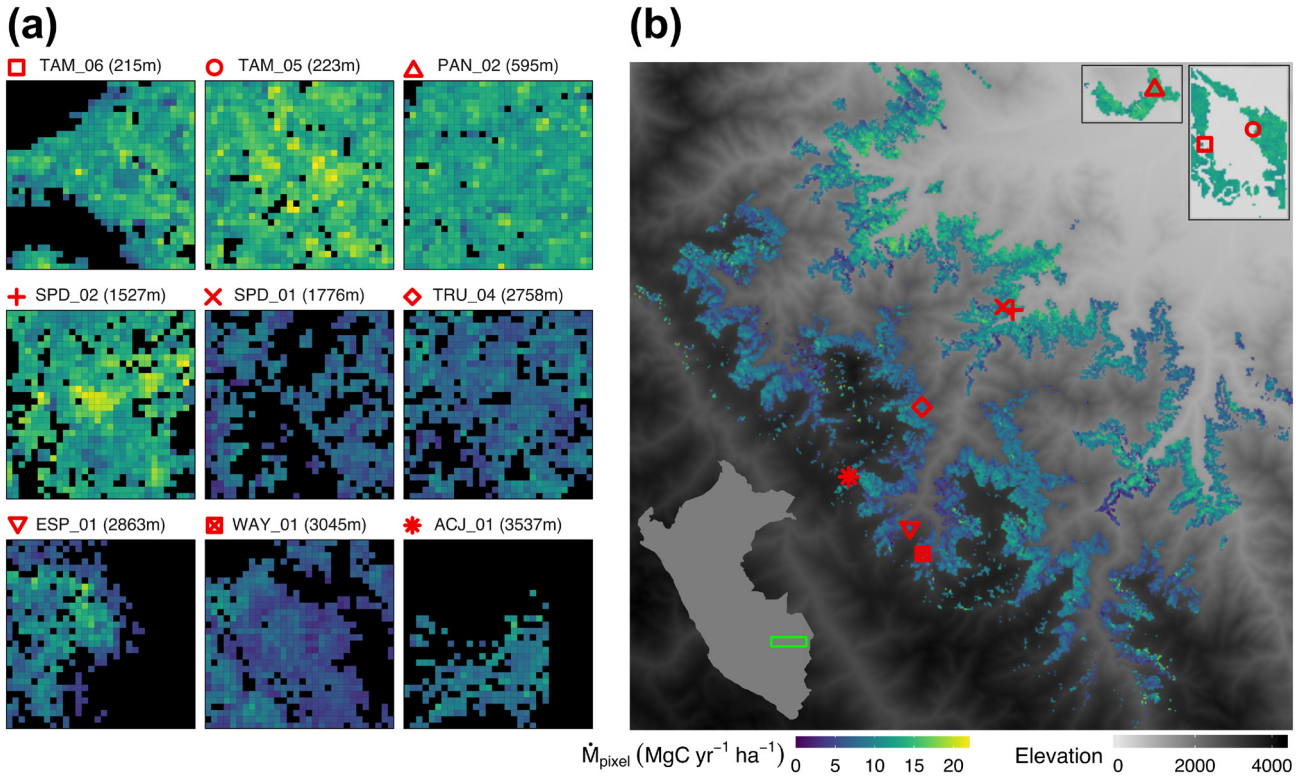Our framework also exposes fundamental links among traits, canopy structure and productivity across a broad

Figure 4. Spatial maps of landscape-scale growth estimates for individual pixels ($\dot{M}_{pixel}$) using our remote sensing canopy functional model (RS-CFM) at (a) 0.01 ha resolution for individual forest plots and (b) 1 ha resolution for 30 040 hectares of forest surrounding the nine focal plots. Boxes in the upper right corner show areas outside the main plot area. Black pixels in plot-level images indicate that no data were available.

temperature/elevation gradient, improving estimates most noticeably in high-productivity, low-elevation forests where canopies are densest (Fig. 2b, Supporting information). This improvement may result from more accurately recreating forest canopy diversity in two ways. First, both MODIS and BESS models represent functional diversity using plant functional types (Running et al. 2004, Zhao et al. 2005, Ryu et al. 2011, Jiang and Ryu 2016), which divides forests into a restricted number of functionally distinct vegetation groups and is common practice in productivity modeling (Purves and Pacala 2008). In contrast, our framework bases functional diversity on remote-sensing measurements of average trait values within individual pixels, better capturing on-the-ground diversity in foliar traits. Second, the MODIS model bases light absorption on total LAI (Running et al. 2004, Zhao et al. 2005), while the BESS model uses a more sophisticated radiative transfer process (Ryu et al. 2011, Jiang and Ryu 2016). Our framework combines LiDAR canopy height measurements for individual pixels with site-specific information about the rate of light extinction as a function of vertical heterogeneity in LAI. The combination of a more complete representation of foliar trait diversity and more precise details about canopy structural diversity – both unique to individual high-resolution pixels – could explain why our RS-CFM captures productivity more accurately, perhaps moving us a step closer to the so-called 'Holy Grail' of plant functional ecology (Lavorel and Garnier 2002).

Although a variety of modeling frameworks have been developed to evaluate primary production at large spatial scales, the remote sensing canopy functional model (RS-CFM) presented here breaks from previous approaches in important ways. First, our model explicitly links plant traits with growth, exposing direct connections between productivity and variation in traits that vary with spatial scale and resolution (Supporting information). This provides a highly flexible model that can be applied across systems, in contrast to models that rely on statistical relationships between variables within a particular dataset, making extrapolation and prediction either challenging or impossible (Scheiter et al. 2013, Fisher et al. 2018, Boisvenue and White 2019). Second, we incorporate spatial variation in functional composition by collecting trait information directly from remote sensing data at high spatial resolution. Although other models (specifically DGVMs) often include remotely-sensed climate data, they typically include indirect estimates of functional variation via established relationships between climate variables and plant functional types (Fisher et al. 2018, Boisvenue and White 2019).

Most importantly, our framework provides a simpler, more mechanistic alternative that provides highly accurate estimates of productivity based on forest functional composition at a given point in time (i.e. without the need for repeated flyovers (Caughlin et al. 2016)). Indeed, on a personal laptop computer with 4 CPU cores, it takes only about 30 s to estimate productivity for the entire region studied here (30 040 ha) at 1 ha resolution. In contrast, DGVMs involve many parameters, sub-models and subroutines that can often take substantial time to run (Quillet et al. 2010, Fisher et al. 2018). Individual-based models track individual trees in a spatially explicit manner that requires lots of information and memory (Larocque et al. 2016, Fisher et al. 2018). These simulation-based models are also evaluated on very short timescales (e.g. hourly as in ED2 (Medvigy et al. 2009)) and often require 'spin-up' periods to equilibrate to initial forest conditions prior to analysis (e.g. 1000 yrs in LPJ-DGVM (Sitch et al. 2003)). These models are attractive, largely because of their attention to such details, but the level of detail comes at considerable computational expense. Thus, improved computational efficiency while maintaining attention to biologically important details are the main advantages of the RS-CFM.

In addition, our framework is flexible and can be easily generalized by including information from other regions beyond the specific choices and calculations we made here for Peruvian tropical forests. For example, it will be interesting to extend the RS-CFM framework to temperate regions – where functional richness is relatively low (Lamanna et al. 2014, Wieczynski et al. 2019) – or regions exhibiting strong gradients in other environmental variables, like precipitation or vapor pressure. To estimate biomass within pixels we use an aggregate allometry that relates biomass to canopy heights and elevation specifically for the wet montane forests of southern Peru (Asner and Mascaro 2014). However, allometric relationships between canopy height and biomass are known to vary and have already been evaluated across regions (Chave et al. 2014, Asner and Mascaro 2014), which can be accommodated in our framework by altering the underlying biomass allometry accordingly.

Because ground-based NPP measurements were originally collected within the same nine focal plots as our plot-scale remote data, we expect our plot-scale NPP estimates to be more representative of the ground-based NPP measurements used in this study than of landscape-scale estimates in general. Given the positive relationship between pixel resolution and NPP estimate accuracy at the plot-scale, it is possible that higher-resolution (0.01 ha) landscape-scale NPP estimates would actually be the most representative of overall regional productivity. However, verifying this requires more extensive ground sampling throughout the region than is currently available. Additionally, although smaller pixels exhibit larger uncertainty due to inherent errors associated with fine-scale remote sensing data, it has been shown that 1 ha resolution remote data for carbon density estimates exhibit 90% agreement with ground-based field estimates (Mascaro et al. 2011, Asner and Mascaro 2014). Conversely, functional richness increases with sampling area (Karadimou et al. 2016, Schneider et al. 2017, Durán et al. 2019), meaning that lower resolution remote data may underestimate trait variation by averaging over larger areas. As a result, lower resolution remote data may only provide accurate growth/NPP estimates at larger spatial scales where more data are available. Consequently, based on this reasoning and our empirical results, we propose more generally that 1 ha-resolution trait and productivity estimates most accurately reflect the true

variation in forests, even across different forests and environments. Further evaluating how these opposing forces produce variation in remote trait and productivity estimates will be an interesting area of future study.

Our analysis identifies $M_L$, $A_L$ and LMA as the strongest contributors to pixel growth rates ($\dot{M}_{pixel}$) while leaf N and P content alone were less influential. This suggests that leaf nutrients affect biomass production mainly through their net impacts on leaf photosynthetic rate. The particular impacts of leaf nutrients on biomass production found here depend on the specific way that these traits were incorporated in our model (i.e. through statistical relationships with multiple components of leaf photosynthetic rate in our study region (Eqn. S8)). In addition to the important impacts of the leaf traits studied here, we argue that future models could be developed to more mechanistically link these and other leaf traits to photosynthetic rates, potentially improving productivity estimates and their sensitivity to variation in forest functional composition.

Furthermore, we use vertical LAI and biomass profiles derived from ground data in the nine focal plots in this study. These components may also vary with study area or the level of disturbance present in a given forest. Such effects could be accounted for by incorporating more sophisticated LiDAR methods that have already been developed to directly measure vertical canopy biomass profiles (Drake et al. 2002, Asner et al. 2012a). Remote sensing technology shows great promise for evaluating this spatial and temporal variation in forest functional composition and productivity (Homolová et al. 2013). We argue that combining elements of our canopy functional model with airborne and satellite remote sensing data (Kampe et al. 2010, Lee et al. 2015, Asner and Martin 2016, Müller et al. 2016, Gamon et al. 2019, Dubayah et al. 2020) has the potential to greatly improve the spatio-temporal acuity of productivity estimates. This information will be especially useful when evaluating the consequences of natural and anthropogenic degradation for the global carbon budget.

Climate change and deforestation are expected to alter the spatial distribution of functional traits expressed within forests (Enquist et al. 2015, Wieczynski et al. 2019). Our framework provides a mechanistic basis for predicting large-scale changes in ecosystem functioning as a result of these expected future disturbances through their effects on trait composition. A first step toward such predictions might be to analyze time-series of remote sensing trait data to establish relationships between changes in functional composition and changes in climate, natural disturbances, anthropogenic impacts, etc. This information can then be combined with mechanistic, trait-based models like ours and extrapolated based on expected future environmental shifts. Analyzing such changes using high-resolution trait and productivity maps will help decode connections between forest composition and NPP, leading to stronger predictions about climate-induced shifts in carbon dynamics, more precise identification of productivity hotspots and more effective management strategies in the future. In this way, directly linking productivity with functional traits and forest structure will not only improve our ability to predict future changes, but will also lead to a deeper understanding of the basic processes driving large-scale patterns in carbon dynamics within and across ecosystems.

## Author contributions

**Daniel J. Wieczynski**: Conceptualization (lead); Data curation (equal); Formal analysis (lead); Investigation (lead); Methodology (lead); Software (lead); Validation (lead); Visualization (lead); Writing – original draft (lead); Writing – review and editing (equal). **Sandra Díaz**: Conceptualization (supporting); Writing – review and editing (supporting). **Sandra M. Durán**: Conceptualization (supporting); Writing – review and editing (supporting). **Nikolaos M. Fyllas**: Conceptualization (supporting); Data curation (supporting); Methodology (supporting); Resources (supporting); Writing – review and editing (supporting). **Norma Salinas**: Conceptualization (supporting); Writing – review and editing (supporting). **Roberta E. Martin**: Conceptualization (supporting); Data curation (equal); Resources (lead); Writing – review and editing (supporting). **Alexander Shenkin**: Conceptualization (supporting); Writing – review and editing (supporting). **Miles R. Silman**: Conceptualization

## Transparent peer review

## Data availability statement

## Supporting information

The Supporting information associated with this article is available with the online version.

## References

Adler, P. B. et al. 2014. Functional traits explain variation in plant life history strategies. – Proc. Natl Acad. Sci. USA 111: 740–745.

Aplin, P. 2005. Remote sensing: ecology. – Prog. Phys. Geogr. Earth Environ. 29: 104–113.

Asner, G. P. and Martin, R. E. 2016. Spectranomics: emerging science and conservation opportunities at the interface of biodiversity and remote sensing. – Global Ecol. Conserv. 8: 212–219.

Asner, G. P. and Mascaro, J. 2014. Mapping tropical forest carbon: calibrating plot estimates to a simple LiDAR metric. – Remote Sens. Environ. 140: 614–624.

Asner, G. P. et al. 2012a. A universal airborne LiDAR approach for tropical forest carbon mapping. – Oecologia 168: 1147–1160.

Asner, G. P. et al. 2012b. Carnegie airborne observatory-2: increasing science data dimensionality via high-fidelity multi-sensor fusion. – Remote Sens. Environ. 124: 454–465.

Asner, G. P. et al. 2015. Quantifying forest canopy traits: imaging spectroscopy versus field survey. – Remote Sens. Environ. 158: 15–27.

Asner, G. P. et al. 2017. Scale dependence of canopy trait distributions along a tropical forest elevation gradient. – New Phytol. 214: 973–988.

Baccini, A. et al. 2017. Tropical forests are a net carbon source based on aboveground measurements of gain and loss. – Science 358: 230–234.

Barlow, J. et al. 2018. The future of hyperdiverse tropical ecosystems. – Nature 559: 517–526.

Boisvenue, C. and White, J. C. 2019. Information needs of next-generation forest carbon models: opportunities for remote sensing science. – Remote Sens. 11: 463.

Bonan, G. B. et al. 2012. Reconciling leaf physiological traits and canopy flux data: use of the TRY and FLUXNET databases in the Community Land Model ver. 4. – J. Geophys. Res. Biogeosci. 117: G2.

Bruelheide, H. et al. 2018. Global trait–environment relationships of plant communities. – Nat. Ecol. Evol. 2: 1906–1917.

Caughlin, T. T. et al. 2016. A hyperspectral image can predict tropical tree growth rates in single-species stands. – Ecol. Appl. 26: 2369–2375.

Chambers, J. Q. et al. 2007. Regional ecosystem structure and function: ecological insights from remote sensing of tropical forests. – Trends Ecol. Evol. 22: 414–423.

Chave, J. et al. 2014. Improved allometric models to estimate the aboveground biomass of tropical trees. – Global Change Biol. 20: 3177–3190.

de Araujo Barbosa, C. C. et al. 2015. Remote sensing of ecosystem services: a systematic review. – Ecol. Indic. 52: 430–443.

Díaz, S. et al. 2016. The global spectrum of plant form and function. – Nature 529: 167–171.

Drake, J. B. et al. 2002. Sensitivity of large-footprint lidar to canopy structure and biomass in a neotropical rainforest. – Remote Sens. Environ. 81: 378–392.

Dubayah, R. et al. 2020. The Global Ecosystem Dynamics Investigation: high-resolution laser ranging of the Earth's forests and topography. – Sci Remote Sens. 1: 100002.

Durán, S. M. et al. 2019. Informing trait-based ecology by assessing remotely sensed functional diversity across a broad tropical temperature gradient. – Sci. Adv. 5: eaaw8114.

Enquist, B. J. et al. 2007. A general integrative model for scaling plant growth, carbon flux and functional trait spectra. – Nature 449: 218–222.

Enquist, B. J. et al. 2015. Chapter Nine – Scaling from traits to ecosystems: developing a general trait driver theory via integrating trait-based and metabolic scaling theories. – In: Pawar, S. et al. (eds), Advances in ecological research. Trait-based ecology – from structure to function. – Academic Press, pp. 249–318.

Fauset, S. et al. 2019. Individual-based modeling of Amazon forests suggests that climate controls productivity while traits control demography. – Front. Earth Sci. 7: 83.

Field, C. B. et al. 1998. Primary production of the biosphere: integrating terrestrial and oceanic components. – Science 281: 237–240.

Fisher, R. A. et al. 2018. Vegetation demographics in earth system models: a review of progress and priorities. – Global Change Biol. 24: 35–54.

Fox, J. and Weisberg, S. 2019. An {R} companion to applied regression, 3rd edn. – Sage Publications, Inc.

Funk, J. L. et al. 2017. Revisiting the Holy Grail: using plant functional traits to understand ecological processes. – Biol. Rev. 92: 1156–1173.

Fyllas, N. M. et al. 2017. Solar radiation and functional traits explain the decline of forest primary productivity along a tropical elevation gradient. – Ecol. Lett. 20: 730–740.

Gamon, J. A. et al. 2019. Assessing vegetation function with imaging spectroscopy. – Surv. Geophys. 40: 489–513.

Gillespie, T. W. et al. 2008. Measuring and modelling biodiversity from space. – Prog. Phys. Geogr. Earth Environ. 32: 203–221.

Goetz, S. and Dubayah, R. 2011. Advances in remote sensing technology and implications for measuring and monitoring forest carbon stocks and change. – Carbon Manage. 2: 231–244.

Gough, C. M. et al. 2019. High rates of primary production in structurally complex forests. – Ecology 100: e02864.

Grace, J. et al. 2014. Perturbations in the carbon budget of the tropics. – Global Change Biol. 20: 3238–3255.

Green, R. O. et al. 1998. Imaging spectroscopy and the airborne visible/infrared imaging spectrometer (AVIRIS). – Remote Sens. Environ. 65: 227–248.

Hilker, T. et al. 2008. The use of remote sensing in light use efficiency based models of gross primary production: a review of current status and future requirements. – Sci. Total Environ. 404: 411–423.

Homolová, L. et al. 2013. Review of optical-based remote sensing for plant trait mapping. – Ecol. Complex. 15: 1–16.

Houborg, R. et al. 2015. Advances in remote sensing of vegetation function and traits. – Int. J. Appl. Earth Obs. Geoinform. 43: 1–6.

Jiang, C. and Ryu, Y. 2016. Multi-scale evaluation of global gross primary productivity and evapotranspiration products derived from Breathing Earth System Simulator (BESS). – Remote Sens. Environ. 186: 528–547.

Kampe, T. U. et al. 2010. NEON: the first continental-scale ecological observatory with airborne remote sensing of vegetation canopy biochemistry and structure. – J. Appl. Remote Sens. 4: 043510.

Karadimou, E. K. et al. 2016. Functional diversity exhibits a diverse relationship with area, even a decreasing one. – Sci. Rep. 6: 35420.

Kattge, J. et al. 2009. Quantifying photosynthetic capacity and its relationship to leaf nitrogen content for global-scale terrestrial biosphere models. – Global Change Biol. 15: 976–991.

Klausmeier, C. A. et al. 2020. Trait-based ecological and eco-evolutionary theory. – In: McCann, K. S. and Gellner, G. (eds), Theoretical ecology: concepts and applications. – Oxford Univ. Press, pp. 161–194.

Lamanna, C. et al. 2014. Functional trait space and the latitudinal diversity gradient. – Proc. Natl Acad. Sci. USA 111: 13745–13750.

Larocque, G. R. et al. 2016. Process-based models: a synthesis of models and applications to address environmental and management issues. – In: Larocque, G. R. (ed.), Ecological forest management handbook. CRC Press, pp. 233–266.

Lausch, A. et al. 2016. Understanding forest health with remote sensing – part I – a review of spectral traits, processes and remote-sensing characteristics. – Remote Sens. 8: 1029.

Lavorel, S. and Garnier, E. 2002. Predicting changes in community composition and ecosystem functioning from plant traits: revisiting the Holy Grail. – Funct. Ecol. 16: 545–556.

Le Toan, T. et al. 2004. Relating radar remote sensing of biomass to modelling of forest carbon budgets. – Clim. Change 67: 379–402.

Lee, C. M. et al. 2015. An introduction to the NASA hyperspectral infrared imager (HyspIRI) mission and preparatory activities. – Remote Sens. Environ. 167: 6–19.

Lim, K. et al. 2003. LiDAR remote sensing of forest structure. – Prog. Phys. Geogr. Earth Environ. 27: 88–106.

Lu, D. 2006. The potential and challenge of remote sensing-based biomass estimation. – Int. J. Remote Sens. 27: 1297–1328.

Madani, N. et al. 2017. Global analysis of bioclimatic controls on ecosystem productivity using satellite observations of solar-induced chlorophyll fluorescence. – Remote Sens. 9: 530.

Malhi, Y. et al. 2017. The variation of productivity and its allocation along a tropical elevation gradient: a whole carbon budget perspective. – New Phytol. 214: 1019–1032.

Martin, A. R. and Thomas, S. C. 2011. A reassessment of carbon content in tropical trees. – PLoS One 6: e23533.

Mascaro, J. et al. 2011. Evaluating uncertainty in mapping forest carbon with airborne LiDAR. – Remote Sens. Environ. 115: 3770–3774.

Medvigy, D. et al. 2009. Mechanistic scaling of ecosystem function and dynamics in space and time: ecosystem demography model ver. 2. – J. Geophys. Res. Biogeosci. 114: G01002.

Mitchard, E. T. A. 2018. The tropical forest carbon cycle and climate change. – Nature 559: 527–534.

Müller, R. et al. 2016. The new hyperspectral sensor DESIS on the multi-payload platform MUSES installed on the ISS. – Int. Arch. Photogramm. Remote Sens. Spat. Inf. Sci. XLI-B1: 461–467.

Nagendra, H. 2001. Using remote sensing to assess biodiversity. – Int. J. Remote Sens. 22: 2377–2400.

Newbold, T. et al. 2012. Mapping functional traits: comparing abundance and presence–absence estimates at large spatial scales. – PLoS One 7: e44019.

Nimon, K. et al. 2020. yhat: interpreting regression effects. R package ver. 2.0-2. – <https://CRAN.R-project.org/package=yhat>.

Pan, Y. et al. 2011. A large and persistent carbon sink in the world's forests. – Science 333: 988–993.

Purves, D. and Pacala, S. 2008. Predictive models of forest dynamics. – Science 320: 1452–1453.

Pury, D. G. G. D. and Farquhar, G. D. 1997. Simple scaling of photosynthesis from leaves to canopies without the errors of big-leaf models. – Plant Cell Environ. 20: 537–557.

Quillet, A. et al. 2010. Toward dynamic global vegetation models for simulating vegetation–climate interactions and feedbacks: recent developments, limitations and future challenges. – Environ. Rev. 18: 333–353.

Ray-Mukherjee, J. et al. 2014. Using commonality analysis in multiple regressions: a tool to decompose regression effects in the face of multicollinearity. – Methods Ecol. Evol. 5: 320–328.

Roy, J. et al. 2001. Terrestrial global productivity. – Academic Press.

Running, S. W. et al. 2004. A continuous satellite-derived measure of global terrestrial primary production. – BioScience 54: 547–560.

Ryu, Y. et al. 2011. Integration of MODIS land and atmosphere products with a coupled-process model to estimate gross primary productivity and evapotranspiration from 1 km to global scales. – Global Biogeochem. Cycles 25: GB4017.

Scheiter, S. et al. 2013. Next-generation dynamic global vegetation models: learning from community ecology. – New Phytol. 198: 957–969.

Schimel, D. et al. 2015. Effect of increasing $CO_2$ on the terrestrial carbon cycle. – Proc. Natl Acad. Sci. USA 112: 436–441.

Schneider, F. D. et al. 2017. Mapping functional diversity from remotely sensed morphological and physiological forest traits. – Nat. Commun. 8: 1441.

Šímová, I. et al. 2015. Shifts in trait means and variances in North American tree assemblages: species richness patterns are loosely related to the functional space. – Ecography 38: 649–658.

Sitch, S. et al. 2003. Evaluation of ecosystem dynamics, plant geography and terrestrial carbon cycling in the LPJ dynamic global vegetation model. – Global Change Biol. 9: 161–185.

Smith, M.-L. et al. 2002. Direct estimation of aboveground forest productivity through hyperspectral remote sensing of canopy nitrogen. – Ecol. Appl. 12: 1286–1302.

Song, C. et al. 2013. Optical remote sensing of terrestrial ecosystem primary productivity. – Prog. Phys. Geogr. Earth Environ. 37: 834–854.

Strigul, N. et al. 2008. Scaling from trees to forests: tractable macroscopic equations for forest dynamics. – Ecol. Monogr. 78: 523–545.

Ustin, S. L. et al. 2004. Using imaging spectroscopy to study ecosystem processes and properties. – BioScience 54: 523–534.

Vane, G. and Goetz, A. F. H. 1988. Terrestrial imaging spectroscopy. – Remote Sens. Environ. 24: 1–29.

Violle, C. et al. 2007. Let the concept of trait be functional! – Oikos 116: 882–892.

Violle, C. et al. 2014. The emergence and promise of functional biogeography. – Proc. Natl Acad. Sci. USA 111: 13690–13696.

Wang, R. and Gamon, J. A. 2019. Remote sensing of terrestrial plant biodiversity. – Remote Sens. Environ. 231: 111218.

Wieczynski, D. J. et al. 2019. Climate shapes and shifts functional biodiversity in forests worldwide. – Proc. Natl Acad. Sci. USA 116: 587–592.

Wieczynski, D. J. et al. 2022. Data from: Improving landscape-scale productivity estimates by integrating trait-based models and remotely-sensed foliar-trait and canopy-structural data. – Dryad Digital Repository, <https://doi.org/10.5061/dryad.s7h44j18n>.

Wright, I. J. et al. 2004. The worldwide leaf economics spectrum. – Nature 428: 821–827.

Yang, Y. et al. 2015. From plant functional types to plant functional traits: a new paradigm in modelling global vegetation dynamics. – Prog. Phys. Geogr. Earth Environ. 39: 514–535.

Zhao, M. et al. 2005. Improvements of the MODIS terrestrial gross and net primary production global data set. – Remote Sens. Environ. 95: 164–176.

Zimble, D. A. et al. 2003. Characterizing vertical forest structure using small-footprint airborne LiDAR. – Remote Sens. Environ. 87: 171–182.